The effects of bioisosteric fluorine in synthetic cannabinoid designer drugs JWH-018, AM-2201, UR-144, XLR-11, PB-22, 5F-PB-22, APICA, and STS-135

Samuel D. Banister, Jordyn Stuart, Richard C. Kevin, Amelia Edington, Mitchell Longworth, Shane M. Wilkinson, Corinne Beinat, Alexandra S. Buchanan, David E. Hibbs, Michelle Glass, Mark Connor, Iain S. McGregor, Michael Kassiou

Contents:

Table S1. Crystal data and structure refinement for UR-144 (**7**).

Identification code	13sam001
Empirical formula	$C_{21}H_{29}NO$
Formula weight	311.45
Temperature/K	150.15
Crystal system	monoclinic
Space group	$P2_1/n$
a/Å	12.1123(8)
b/Å	10.7990(7)
c/Å	13.9200(9)
α/°	90.00
β/°	93.6870(10)
γ/°	90.00
Volume/Å^3	1817.0(2)
Z	4
ρ_{calc}mg/mm^3	1.139
m/mm^{-1}	0.069
F(000)	680.0
Crystal size/mm^3	0.15 × 0.15 × 0.1
2Θ range for data collection	4.32 to 56.5°
Index ranges	$-15 \leq h \leq 15$, $-14 \leq k \leq 12$, $-18 \leq l \leq 18$
Reflections collected	13869
Independent reflections	4170[R(int) = 0.0179]
Data/restraints/parameters	4170/0/213
Goodness-of-fit on F^2	1.050
Final R indexes [I>=2σ (I)]	$R_1 = 0.0398$, $wR_2 = 0.1019$
Final R indexes [all data]	$R_1 = 0.0478$, $wR_2 = 0.1077$
Largest diff. peak/hole / e Å^{-3}	0.26/-0.20

Table S2. Fractional Atomic Coordinates ($\times 10^4$) and Equivalent Isotropic Displacement Parameters ($Å^2 \times 10^3$) for UR-144 (**7**). U_{eq} is defined as 1/3 of of the trace of the orthogonalised U_{IJ} tensor.

Atom	**x**	**y**	**z**	**U_{eq}**
C1	11919.5(8)	1638.6(10)	2202.6(8)	23.7(2)
C2	11397.0(8)	2299.5(10)	1453.3(7)	22.7(2)
C3	12215.4(8)	3151.2(10)	1127.1(7)	22.4(2)
C4	13188.4(9)	2957.9(10)	1724.8(7)	22.8(2)
C5	14152.5(9)	3646.4(11)	1637.8(8)	26.2(2)
C6	14131.6(9)	4538.8(11)	927.6(8)	28.9(2)
C7	13181.9(10)	4735.9(11)	314.8(8)	29.7(3)
C8	12224.0(9)	4056(1)	402.3(8)	26.5(2)
C9	10242.0(9)	2202.4(10)	1073.1(8)	24.2(2)
C10	9547.6(8)	1249.8(10)	1517.4(8)	23.7(2)
C11	8620.4(8)	515.2(10)	959.5(8)	25.3(2)
C12	8318.1(8)	1442.5(11)	1706.8(8)	25.4(2)
C13	8361.6(10)	779.1(13)	-100.5(8)	34.5(3)
C14	8560.5(10)	-862.5(11)	1166.9(10)	33.0(3)
C15	7739.9(10)	2632.3(12)	1396.0(9)	33.4(3)
C16	7986.8(10)	1007.4(12)	2684.7(9)	33.0(3)
C17	13790.9(9)	1480.2(11)	3079.5(8)	28.3(2)
C18	14695.4(9)	744.0(11)	2618.3(9)	31.0(3)
C19	14273.7(10)	-156.0(11)	1838.3(9)	30.8(3)
C20	15187.5(11)	-962.6(13)	1475.6(10)	41.2(3)
C21	14809.3(14)	-1804.2(15)	646.8(12)	53.1(4)
N1	12982.9(7)	2027.3(9)	2374.1(6)	23.9(2)
O1	9888.8(7)	2895.1(8)	422.0(6)	34.0(2)

Table S3. Bond lengths [Å] for UR-144 (**7**).

Atom	**Atom**	**Length/Å**
C1	C2	1.3830(15)
C1	N1	1.3611(13)
C2	C3	1.4465(14)
C2	C9	1.4674(14)
C3	C4	1.4138(15)
C3	C8	1.4051(15)
C4	C5	1.3962(15)
C4	N1	1.3848(14)
C5	C6	1.3797(16)
C6	C7	1.4036(17)
C7	C8	1.3849(16)
C9	C10	1.4882(15)
C9	O1	1.2306(13)
C10	C11	1.5432(14)
C10	C12	1.5430(14)
C11	C12	1.5059(15)
C11	C13	1.5157(16)
C11	C14	1.5181(16)
C12	C15	1.5131(16)
C12	C16	1.5183(16)
C17	C18	1.5281(16)
C17	N1	1.4654(13)
C18	C19	1.5209(17)
C19	C20	1.5200(17)
C20	C21	1.516(2)

Table S4. Bond angles [deg] for UR-144 (**7**).

Atom	Atom	Atom	Angle/°
N1	C1	C2	110.80(9)
C1	C2	C3	105.98(9)
C1	C2	C9	127.92(10)
C3	C2	C9	126.08(10)
C4	C3	C2	106.47(9)
C8	C3	C2	134.79(10)
C8	C3	C4	118.74(10)
C5	C4	C3	122.72(10)
N1	C4	C3	108.25(9)
N1	C4	C5	129.02(10)
C6	C5	C4	117.21(10)
C5	C6	C7	121.19(10)
C8	C7	C6	121.65(10)
C7	C8	C3	118.47(10)
C2	C9	C10	116.79(9)
O1	C9	C2	120.03(10)
O1	C9	C10	123.18(10)
C9	C10	C11	123.97(9)
C9	C10	C12	123.72(9)
C12	C10	C11	58.41(7)
C12	C11	C10	60.79(7)
C12	C11	C13	120.21(10)
C12	C11	C14	120.24(10)
C13	C11	C10	119.44(9)
C13	C11	C14	111.10(10)
C14	C11	C10	116.76(9)
C11	C12	C10	60.80(7)
C11	C12	C15	119.72(10)
C11	C12	C16	120.23(10)
C15	C12	C10	119.98(10)
C15	C12	C16	112.02(10)
C16	C12	C10	115.16(9)
N1	C17	C18	113.22(9)
C19	C18	C17	114.55(9)
C20	C19	C18	112.64(10)
C21	C20	C19	113.92(12)
C1	N1	C4	108.49(9)
C1	N1	C17	125.23(9)
C4	N1	C17	126.12(9)

Table S5. Anisotropic Displacement Parameters ($Å^2 \times 10^3$) for UR-144 (**7**). The Anisotropic displacement factor exponent takes the form: $-2\pi^2[h^2a^{*2}U_{11}+...+2hka \times b \times U_{12}]$

Atom	U_{11}	U_{22}	U_{33}	U_{23}	U_{13}	U_{12}
C1	21.2(5)	23.5(5)	26.7(5)	-0.5(4)	3.3(4)	-2.4(4)
C2	22.3(5)	21.3(5)	24.6(5)	-0.8(4)	3.1(4)	-0.9(4)
C3	22.8(5)	20.9(5)	23.7(5)	-3.4(4)	3.9(4)	-0.4(4)
C4	23.6(5)	21.9(5)	23.4(5)	-1.9(4)	4.9(4)	-0.4(4)
C5	23.1(5)	28.1(6)	27.7(5)	-3.9(4)	3.5(4)	-3.7(4)
C6	28.3(6)	27.4(6)	32.0(6)	-3.3(4)	9.9(4)	-6.9(4)
C7	35.1(6)	26.1(6)	28.9(6)	2.7(4)	9.9(4)	-2.0(5)
C8	28.4(5)	25.6(6)	25.7(5)	0.3(4)	3.8(4)	1.4(4)
C9	22.7(5)	24.4(5)	25.6(5)	-0.8(4)	1.9(4)	0.4(4)
C10	18.4(5)	25.5(5)	27.0(5)	2.4(4)	-0.9(4)	0.1(4)
C11	18.9(5)	27.2(6)	29.6(5)	-2.3(4)	0.6(4)	-0.5(4)
C12	18.4(5)	28.5(6)	29.0(5)	-1.9(4)	0.6(4)	-0.6(4)
C13	33.0(6)	40.9(7)	29.2(6)	-3.8(5)	-1.2(5)	-4.9(5)
C14	26.2(6)	28.2(6)	44.7(7)	-2.5(5)	2.1(5)	-3.1(5)
C15	26.4(6)	31.8(6)	41.9(7)	-3.1(5)	0.5(5)	6.2(5)
C16	26.9(6)	40.9(7)	31.6(6)	-1.8(5)	5.6(4)	-4.7(5)
C17	25.1(5)	33.9(6)	25.2(5)	2.8(4)	-3.6(4)	-1.1(5)
C18	24.2(5)	33.8(6)	34.2(6)	1.8(5)	-4.3(4)	1.9(5)
C19	28.6(6)	29.1(6)	34.1(6)	2.4(5)	-2.5(4)	2.0(5)
C20	40.3(7)	39.7(7)	42.9(7)	-1.6(6)	-3.7(5)	13.2(6)
C21	62.4(10)	43.9(9)	52.5(9)	-10.3(7)	0.4(7)	11.6(7)
N1	20.7(4)	25.6(5)	25.4(4)	1.5(4)	1.3(3)	-1.5(3)
O1	28.5(4)	36.6(5)	36.2(4)	11.6(4)	-3.1(3)	-1.8(3)

Table S6. Hydrogen Atom Coordinates ($Å \times 10^4$) and Isotropic Displacement Parameters ($Å^2 \times 10^3$) for UR-144 (**7**).

Atom	x	y	z	U(eq)
H1	11582	1000	2550	28
H5	14796	3506	2050	31
H6	14772	5029	852	35
H7	13196	5351	-172	36
H8	11587	4198	-18	32
H10	9961	752	2028	28
H13A	8391	1674	-213	52
H13B	7619	471	-295	52
H13C	8906	363	-479	52
H14A	9105	-1301	802	50
H14B	7817	-1169	975	50
H14C	8721	-1007	1857	50
H15A	7850	3252	1908	50
H15B	6947	2474	1271	50
H15C	8049	2941	808	50
H16A	8453	306	2900	49
H16B	7209	750	2635	49
H16C	8085	1686	3150	49
H17A	13399	926	3511	34
H17B	14140	2150	3479	34
H18A	15211	1333	2337	37
H18B	15120	274	3128	37
H19A	13701	-694	2097	37
H19B	13923	318	1291	37
H20A	15786	-421	1267	49
H20B	15500	-1478	2015	49
H21A	14517	-1302	102	80
H21B	14229	-2359	851	80
H21C	15437	-2296	452	80

Table S7. Torsion angles [deg] for UR-144 (**7**).

A	B	C	D	Angle/°
C1	C2	C3	C4	-1.06(11)
C1	C2	C3	C8	179.50(12)
C1	C2	C9	C10	-2.38(16)
C1	C2	C9	O1	177.17(11)
C2	C1	N1	C4	-0.60(12)
C2	C1	N1	C17	-176.30(10)
C2	C3	C4	C5	-178.22(10)
C2	C3	C4	N1	0.73(11)
C2	C3	C8	C7	178.30(11)
C2	C9	C10	C11	-145.83(10)
C2	C9	C10	C12	142.21(10)
C3	C2	C9	C10	179.69(10)
C3	C2	C9	O1	-0.75(17)
C3	C4	C5	C6	-0.51(16)
C3	C4	N1	C1	-0.11(12)
C3	C4	N1	C17	175.54(10)
C4	C3	C8	C7	-1.08(15)
C4	C5	C6	C7	-0.51(16)
C5	C4	N1	C1	178.75(11)
C5	C4	N1	C17	-5.60(18)
C5	C6	C7	C8	0.73(17)
C6	C7	C8	C3	0.10(17)
C8	C3	C4	C5	1.33(16)
C8	C3	C4	N1	-179.73(9)
C9	C2	C3	C4	177.24(10)
C9	C2	C3	C8	-2.20(19)
C9	C10	C11	C12	-111.81(11)
C9	C10	C11	C13	-1.54(16)
C9	C10	C11	C14	136.82(11)
C9	C10	C12	C11	112.22(11)
C9	C10	C12	C15	2.74(16)
C9	C10	C12	C16	-135.77(11)
C10	C11	C12	C15	109.88(11)
C10	C11	C12	C16	-103.77(11)
C11	C10	C12	C15	-109.47(11)
C11	C10	C12	C16	112.01(11)
C12	C10	C11	C13	110.27(12)
C12	C10	C11	C14	-111.37(11)
C13	C11	C12	C10	-109.03(11)
C13	C11	C12	C15	0.86(15)
C13	C11	C12	C16	147.21(11)
C14	C11	C12	C10	105.73(11)

C14	C11	C12	C15	-144.39(11)
C14	C11	C12	C16	1.97(15)
C17	C18	C19	C20	-173.93(10)
C18	C17	N1	C1	108.19(12)
C18	C17	N1	C4	-66.76(14)
C18	C19	C20	C21	-175.75(12)
N1	C1	C2	C3	1.04(12)
N1	C1	C2	C9	-177.22(10)
N1	C4	C5	C6	-179.22(10)
N1	C17	C18	C19	-47.60(14)
O1	C9	C10	C11	34.63(16)
O1	C9	C10	C12	-37.32(16)

Figure S1. ^{1}H NMR spectrum (500 MHz, $CDCl_3$, 300 K) of XLR-11 (**8**).

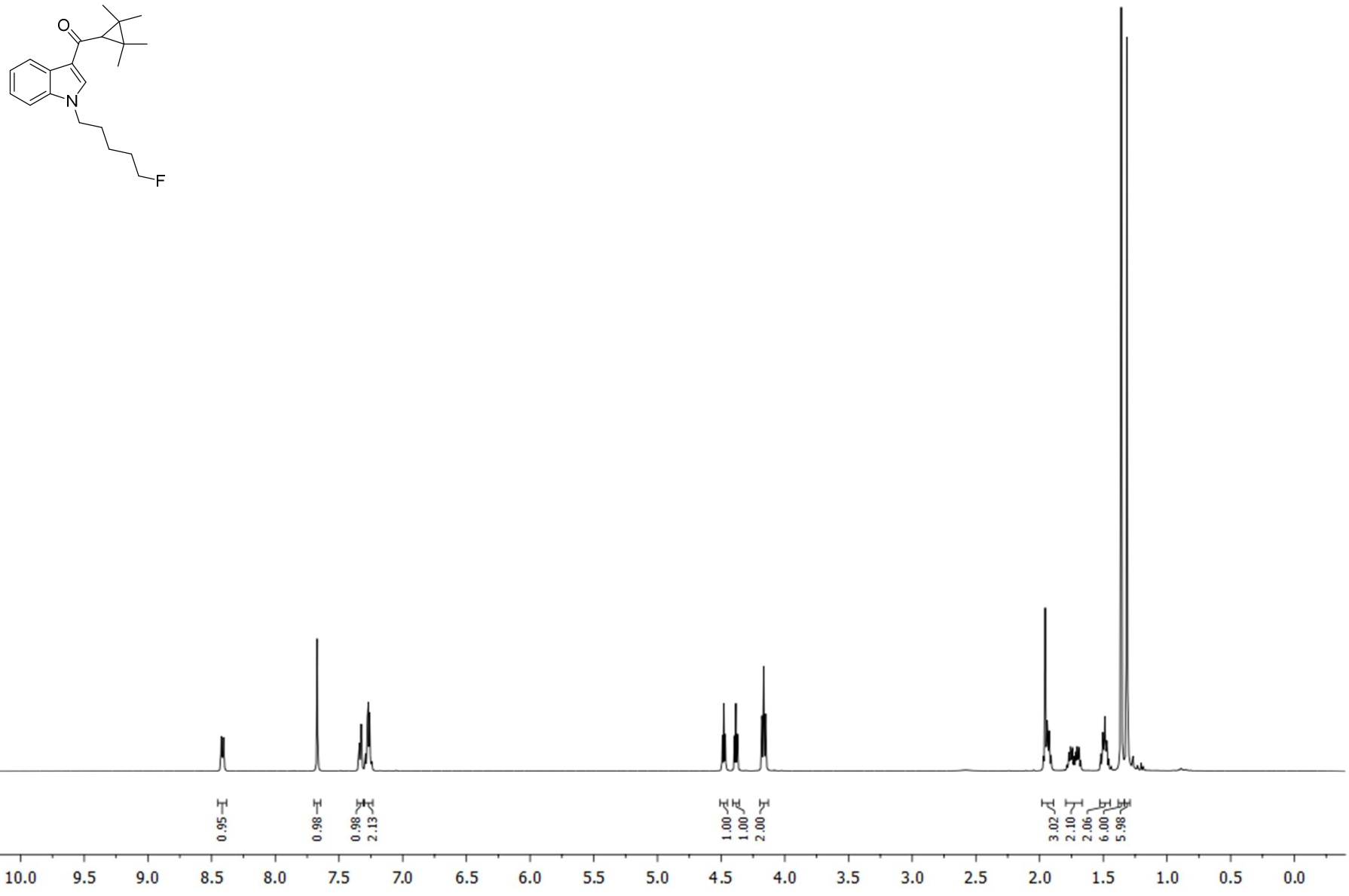

Figure S2. ^{13}C NMR spectrum (125 MHz, $CDCl_3$, 300 K) of XLR-11 (**8**).

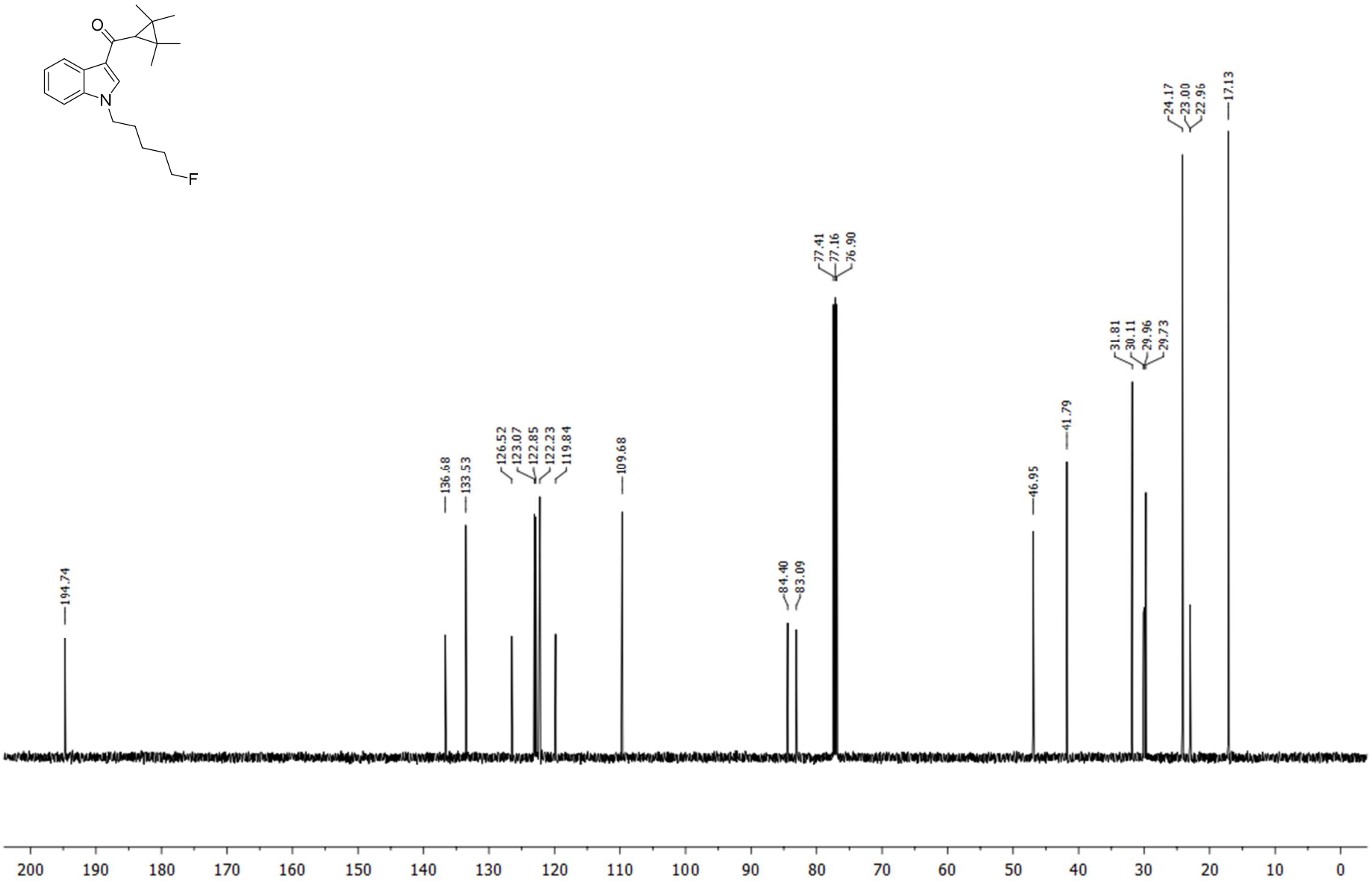

Figure S3. ^{1}H NMR spectrum (500 MHz, $CDCl_3$, 300 K) of STS-135 (**13**).

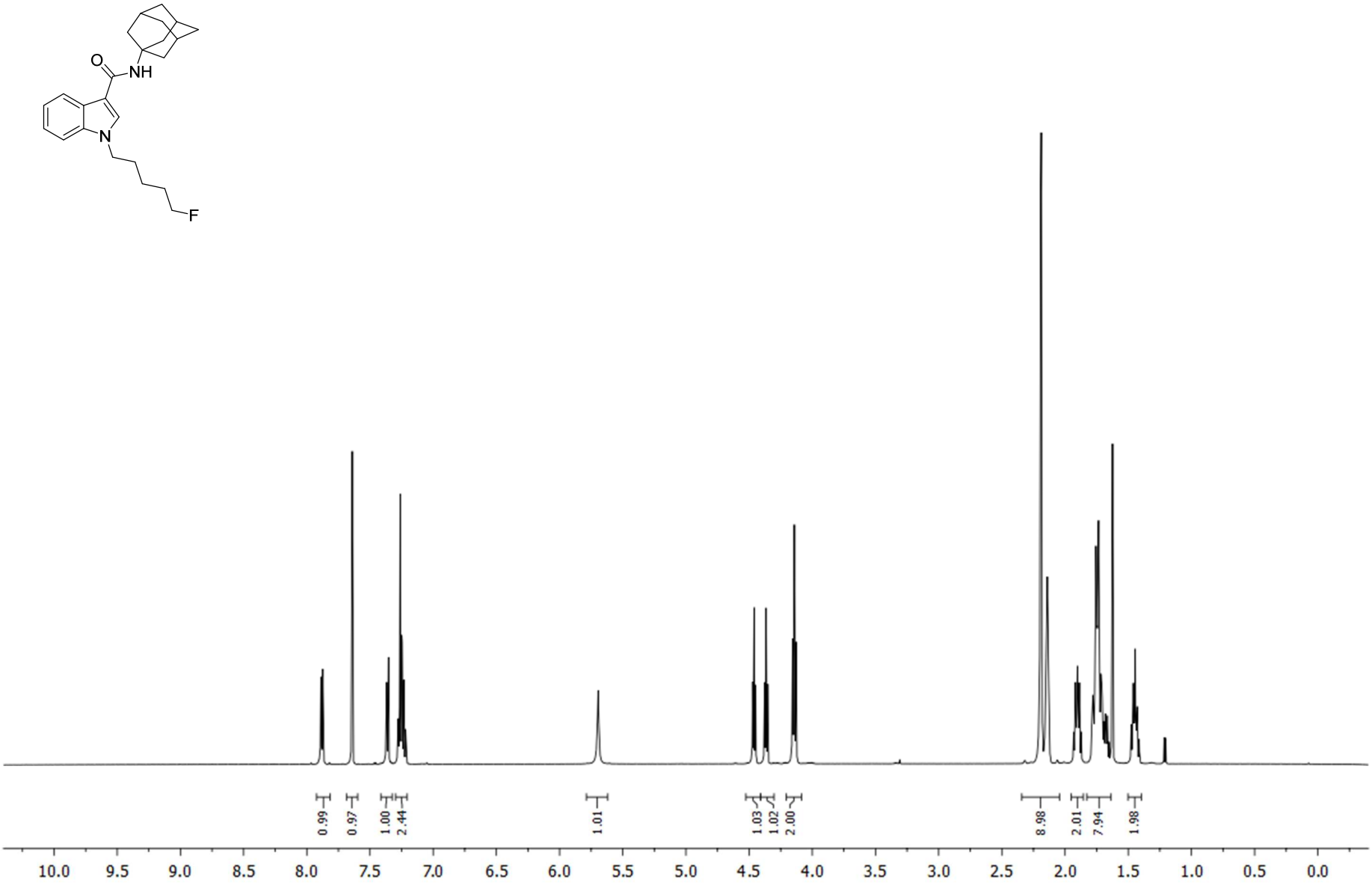

Figure S4. ^{13}C NMR spectrum (125 MHz, $CDCl_3$, 300 K) of STS-135 (**13**).

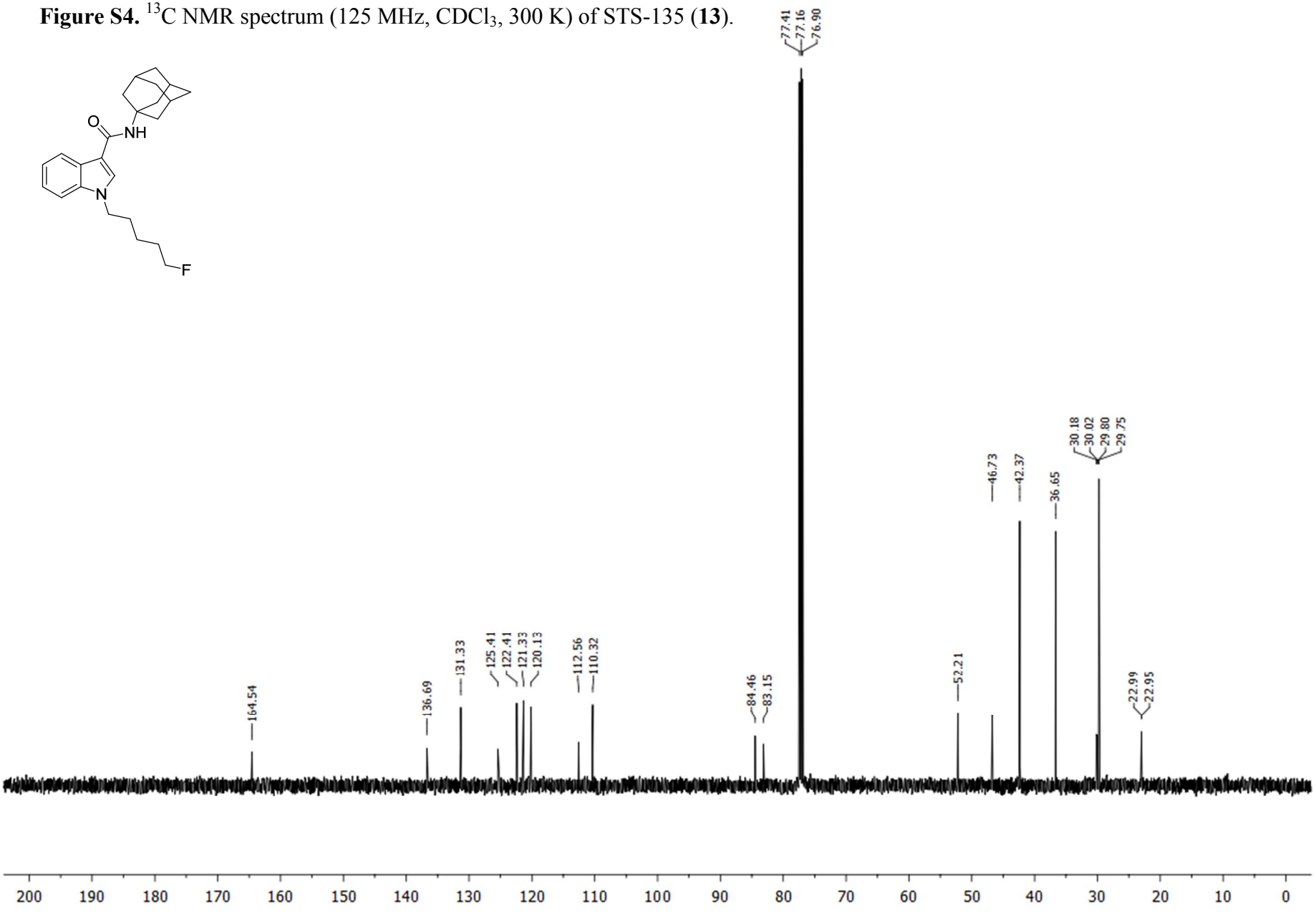

Figure S5. Mean maximal decrease in body temperature (+/- SEM) for all compounds tested *in vivo*

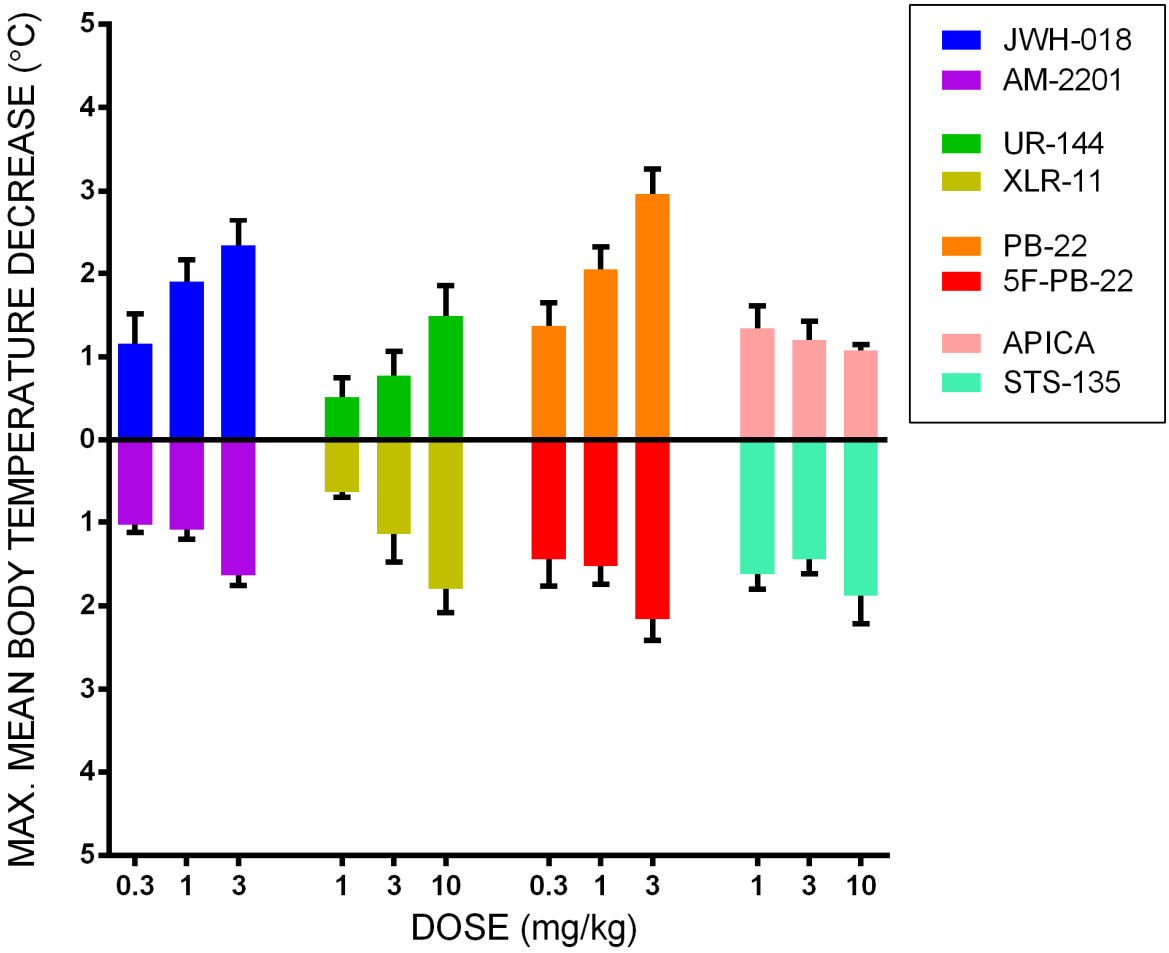

The body temperature data for individual rats during the 6 h post-drug was examined to determine the lowest body temperature datapoint recorded. The body temperature recorded during vehicle treatment at that same time point was then used to calculate body temperature change. This was averaged across all the rats receiving the same drug and dose to produce Figure 5. In this Figure compounds are presented in pairs, with the non-fluorinated compound extending upwards and the fluorinated compound downwards.

The data obtained for maximal body temperature change were compared between each drug pair using two-way mixed model ANOVAs, with drug-treatment as the between-subjects factor, and dose as the within-subjects factor. There was a significant main effect of dose for every drug pair (all $p < .05$). However there was no main effect of drug-treatment for any drug pair (all $p > .05$). Bonferroni contrasts comparing each dose for each pair (e.g. JWH-018 0.3 mg/kg – AM-2201 0.3 mg/kg) revealed no significant difference for any drug pair at any dose (all $p > .05$).

Figure S6. Mean area under the curve (AUC +/- SEM) for body temperature for each compound and dose tested, expressed as a percentage of that obtained with PB-22.

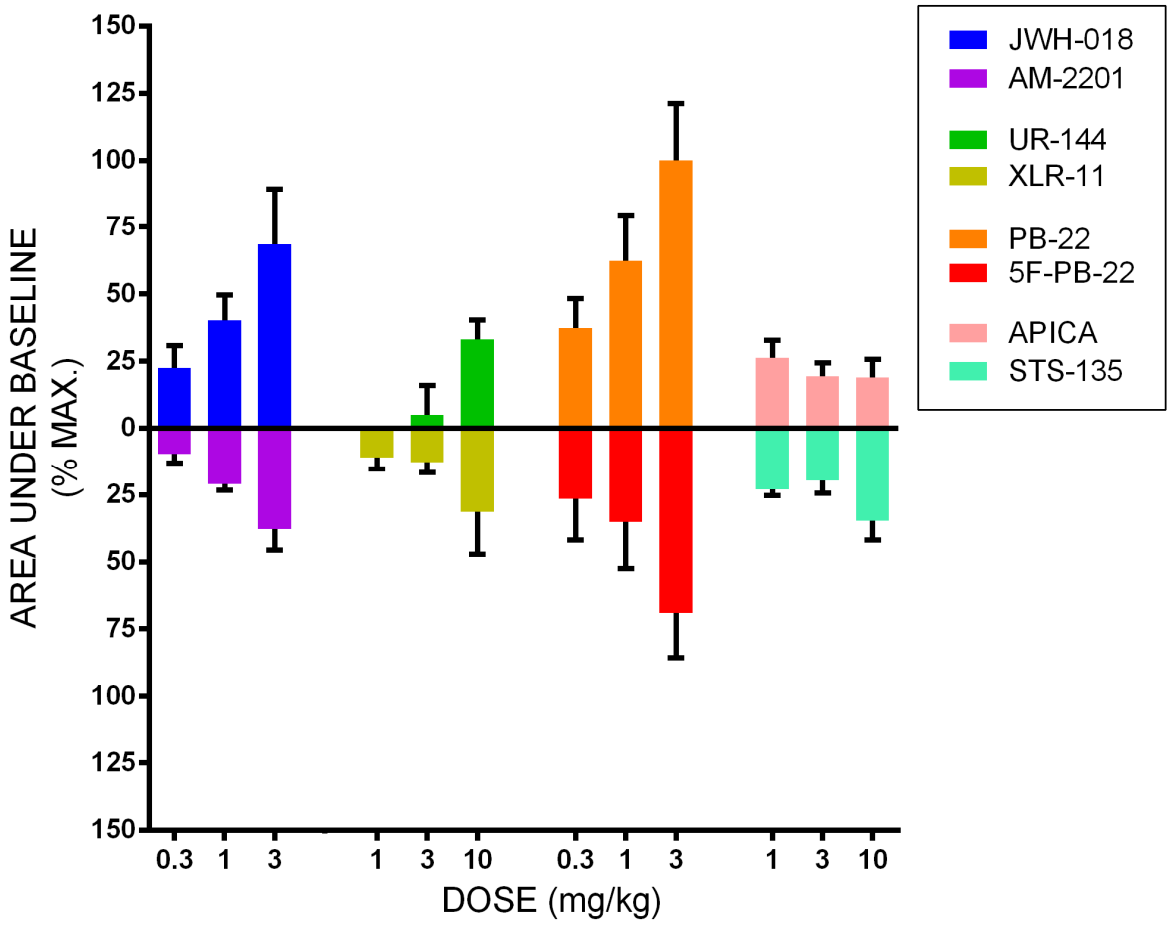

The mean area under each drug-treatment curve, relative to baseline under vehicle treatment, was calculated and normalized relative to the highest observed AUC (obtained with 3 mg/kg PB-22). Compounds are presented in pairs, with the fluorinated compound extending downwards.

These areas were calculated via the trapezoidal method. Briefly, for any time point, the area between baseline data points (B_t) and drug-treatment data points (D_t) and the next time points (B_{t+1} and D_{t+1}) forms a trapezoid, the area of which can be calculated via the formula:

$$Area = \frac{(B_t - D_t) + (B_{t+1} - D_{t+1})}{2}$$

These areas were summed from the time of injection to 6 hours post-injection.

The mean area for body temperature between baseline and drug-treatment for each drug pair was analysed using two-way mixed model ANOVAs, with drug-treatment as the between subjects factor, and dose as the within subjects factor. Similarly to peak body temperature decrease, there was a significant main effect of dose for every drug pair (all $p < .05$). However there was no main effect of drug-treatment for any drug pair (all $p > .05$). Bonferroni contrasts comparing

each dose for each pair revealed no significant difference for any drug pair at any dose (all $p > .05$).

These results suggest that terminal fluorination has no overall effect on potency as measured by body temperature. However, it remains possible that other measures (e.g. cognitive function, analgesia, appetite) may be differentially affected as a function of fluorination. Further behavioural testing is necessary to clarify this issue.

Ranking the AUCs for all eight compounds at the 3 mg/kg dose gave the following ranking: PB-22 > 5F-PB-22 = JWH-018 > AM-2201 > APICA = STS-135 = XLR-11 > UR-144.

Table S8. Binding affinities and functional activities of selected cannabinoids at CB_1 and CB_2 receptors.

Compound	CB_1 EC_{50} (nM)	CB_2 EC_{50} (nM)	CB_1 K_i (nM)	CB_2 K_i (nM)	Ref
1 (Δ^9-THC)	250	1157	35.3	3.9	1
			39.5	40	2
			40.7	36.4	3
			53.5	75.3	4
			80.3	32.2	5
3 (WIN 55,212-2)	284	62	1.89	0.28	3
			4.4	1.2	6
			9.94	16.2	1
			62.3	3.3	4
			123	4.1	7
4 (JWH-018)	102	133	9.00	2.94	8
5 (AM-2201)	38	58	1	2.6	9
7 (UR-144)	421	72	150	1.8	10
			29	4.5	11
8 (XLR-11)	98	83	24	2.1	11
9 (5-OH-UR-144)	1959	6.5	680	0.71	10
12 (APICA)	128	29	175[a]	176[a]	12

[a] IC_{50} (nM)

References

1. Rinaldi-Carmona, M.; Barth, F.; Héaulme, M.; Shire, D.; Calandra, B.; Congy, C.; Martinez, S.; Maruani, J.; Néliat, G.; Caput, D.; Ferrara, P.; Soubrié, P.; Brelière, J. C.; Le Fur, G. SR141716A, a potent and selective antagonist of the brain cannabinoid receptor. *FEBS Letters* **1994,** *350* (2–3), 240-244.

2. Bayewitch, M.; Rhee, M. H.; Avidor-Reiss, T.; Breuer, A.; Mechoulam, R.; Vogel, Z. (-)-Delta9-tetrahydrocannabinol antagonizes the peripheral cannabinoid receptor-mediated inhibition of adenylyl cyclase. *J. Biol. Chem.* **1996,** *271* (17), 9902-5.

3. Showalter, V. M.; Compton, D. R.; Martin, B. R.; Abood, M. E. Evaluation of binding in a transfected cell line expressing a peripheral cannabinoid receptor (CB2): identification of cannabinoid receptor subtype selective ligands. *J. Pharmacol. Exp. Ther.* **1996,** *278* (3), 989-99.

4. Felder, C. C.; Joyce, K. E.; Briley, E. M.; Mansouri, J.; Mackie, K.; Blond, O.; Lai, Y.; Ma, A. L.; Mitchell, R. L. Comparison of the pharmacology and signal transduction of the human cannabinoid CB1 and CB2 receptors. *Mol. Pharmacol.* **1995,** *48* (3), 443-50.

5. Rhee, M. H.; Vogel, Z.; Barg, J.; Bayewitch, M.; Levy, R.; Hanus, L.; Breuer, A.; Mechoulam, R. Cannabinol derivatives: binding to cannabinoid receptors and inhibition of adenylylcyclase. *J. Med. Chem.* **1997,** *40* (20), 3228-33.

6. Hillard, C. J.; Manna, S.; Greenberg, M. J.; DiCamelli, R.; Ross, R. A.; Stevenson, L. A.; Murphy, V.; Pertwee, R. G.; Campbell, W. B. Synthesis and Characterization of Potent and Selective Agonists of the Neuronal Cannabinoid Receptor (CB1). *J. Pharmacol. Exp. Ther.* **1999,** *289* (3), 1427-1433.

7. Shire, D.; Calandra, B.; Rinaldi-Carmona, M.; Oustric, D.; Pessegue, B.; Bonnin-Cabanne, O.; Le Fur, G.; Caput, D.; Ferrara, P. Molecular cloning, expression and function of the murine CB2 peripheral cannabinoid receptor. *Biochim. Biophys. Acta* **1996,** *1307* (2), 132-6.

8. Aung, M. M.; Griffin, G.; Huffman, J. W.; Wu, M. J.; Keel, C.; Yang, B.; Showalter, V. M.; Abood, M. E.; Martin, B. R. Influence of the N-1 alkyl chain length of cannabimimetic indoles upon CB1 and CB2 receptor binding. *Drug Alcohol Depen.* **2000,** *60* (2), 133-140.

9. Makriyannis, A.; Deng, H. Preparation of cannabimimetic indole derivatives with cannabinoid CB1 or CB2 receptor binding affinity. World patent WO 2001/028557, 26 April, 2001.

10. Frost, J. M.; Dart, M. J.; Tietje, K. R.; Garrison, T. R.; Grayson, G. K.; Daza, A. V.; El-Kouhen, O. F.; Yao, B. B.; Hsieh, G. C.; Pai, M.; Zhu, C. Z.; Chandran, P.; Meyer, M. D. Indol-3-ylcycloalkyl ketones: effects of N1 substituted indole side chain variations on CB(2) cannabinoid receptor activity. *J. Med. Chem.* **2010,** *53* (1), 295-315.

11. Wiley, J. L.; Marusich, J. A.; Lefever, T. W.; Grabenauer, M.; Moore, K. N.; Thomas, B. F. Cannabinoids in disguise: Delta9-tetrahydrocannabinol-like effects of tetramethylcyclopropyl ketone indoles. *Neuropharmacology* **2013,** *75*, 145-54.

12. Uchiyama, N.; Kawamura, M.; Kikura-Hanajiri, R.; Goda, Y. URB-754: A new class of designer drug and 12 synthetic cannabinoids detected in illegal products. *Forensic Sci. Int.* **2013,** *227* (1-3), 21-32.